NASA TECHNICAL NOTE

NASA TN D-2963

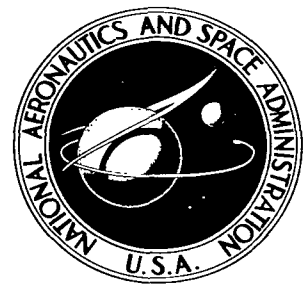

COVERAGE DIAGRAMS FOR X-Y AND ELEVATION-OVER-AZIMUTH ANTENNA MOUNTS

by Chesley H. Looney, Jr., and Donald J. Carlson

Goddard Space Flight Center
Greenbelt, Md.

NATIONAL AERONAUTICS AND SPACE ADMINISTRATION • WASHINGTON, D. C. • AUGUST 1965

COVERAGE DIAGRAMS FOR X-Y AND ELEVATION-OVER-AZIMUTH ANTENNA MOUNTS

By Chesley H. Looney, Jr., and Donald J. Carlson

Goddard Space Flight Center
Greenbelt, Md.

NATIONAL AERONAUTICS AND SPACE ADMINISTRATION

For sale by the Clearinghouse for Federal Scientific and Technical Information
Springfield, Virginia 22151 – Price $1.00

COVERAGE DIAGRAMS FOR X-Y AND ELEVATION-OVER-AZIMUTH ANTENNA MOUNTS

by
Chesley H. Looney, Jr. and Donald J. Carlson
Goddard Space Flight Center

SUMMARY

At any satellite tracking station, there will occur certain satellite passes which require that the primary-axis shaft of a two-axis antenna mount move at very great speeds (up to infinity) to maintain continuous tracking coverage. Since the speed capability of a shaft is always limited to some finite value, there will be some loss of coverage on those passes which require speeds in excess of the shaft's actual capability. In addition, there may be mechanical limits to the motions of axes which prevent the antenna from scanning the whole hemisphere above the horizon. The losses of coverage for X-Y and elevation-over-azimuth (AZ-EL) antenna mounts are considered in this paper, and it is concluded that the two types of mounts do not differ significantly with respect to the percentage of data lost as a result of shaft speed limitations; however, the relative advantage of the X-Y mount is the fact that the data which it loses is of poor quality, while that lost by the AZ-EL mount is of the best quality.

CONTENTS

COVERAGE DIAGRAMS FOR X-Y AND ELEVATION-OVER-AZIMUTH ANTENNA MOUNTS

by
Chesley H. Looney, Jr. and Donald J. Carlson
Goddard Space Flight Center

INTRODUCTION

A previously-published paper* gives the background basic description of X-Y and elevation-over-azimuth (AZ-EL) mounts, and makes comparisons of the maximum shaft speeds required for tracking satellites. Since the maximum speed capability of a primary axis is finite, there will always be some loss of coverage due to the fact that on some passes of a satellite, the speed required for tracking will exceed the speed capability of the axis. In addition, there may be mechanical limits to the motions of the axes which prevent the antenna from scanning the whole hemisphere above the horizon. The losses of coverage resulting from these factors are considered in this paper.

REQUIRED MAXIMUM SHAFT SPEEDS

Two satellites, each in its own circular orbit at a height of 100 nautical miles, are shown in Figure 1. At the moment depicted by the figure, both satellites lie in the meridian plane (the plane of the figure) and are traveling directly eastward at the circular-orbit speed.

Satellite J is being tracked by an elevation-over-azimuth antenna located at the tracking station, and satellite K is being tracked by an X-Y antenna located at the same station. The elevation angles of the respective satellites are such as to require equal shaft speeds (viz., 3 deg/sec) on the primary axes (azimuth axis and X axis) of the two antenna mounts.

Figure 2 is similar to Figure 1, except that it depicts satellites P and Q in 600 n. mi. circular orbits.

On a given pass of a satellite in a near-earth orbit, the maximum speed required of a primary-axis shaft always occurs at the time when the satellite is at the minimum distance from the axis.

*Rolinski, A. J., Carlson, D. J., and Coates, R. J., "Satellite-Tracking Characteristics of the X-Y Mount for Data Acquisition Antennas", NASA Technical Note D-1697, June 1964.

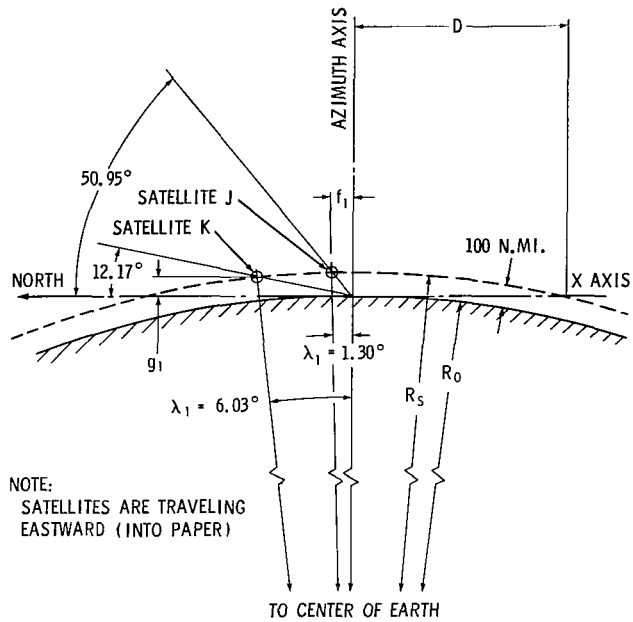

Figure 1—Satellite positions for $\dot{A}_{max}$ = 3 deg/sec and for $\dot{X}_{max}$ = 3 deg/sec; 100 n. mi. circular orbits.

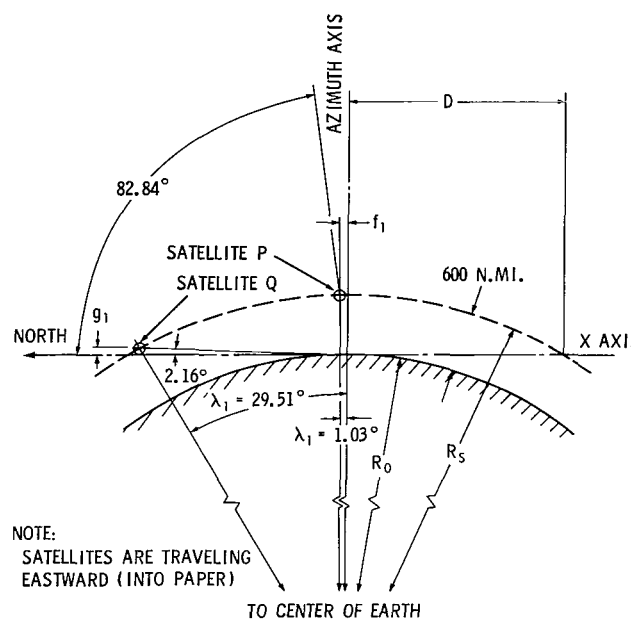

Figure 2—Satellite positions for $\dot{A}_{max}$ = 3 deg/sec and for $\dot{X}_{max}$ = 3 deg/sec; 600 n. mi. circular orbits.

For an azimuth axis, this is the time at which the satellite reaches its maximum elevation angle, and the magnitude of the maximum required shaft speed is essentially independent of the azimuth pointing direction of the satellite's velocity vector. For an X axis, on the other hand, the maximum shaft speed requirement occurs at the time when the satellite crosses the station meridian, and the magnitude of the shaft speed requirement is dependent upon the azimuth pointing direction of the velocity vector.

The magnitudes of the maximum required speeds of the azimuth and X axes may be expressed in terms of the angles and distances shown in Figure 1, as follows:

Let the time of minimum distance from a primary axis be designated by the subscript 1. Then, from Figure 1, it is evident that the maximum azimuth-axis speed and the maximum X-axis speed required to track a satellite on a particular pass are respectively,

$$\dot{A}_{max} = \frac{V_1}{f_1} = \frac{V_1}{R_s \sin \lambda_1} \tag{1}$$

and

$$\dot{X}_{max} = \frac{V_1 \sin B_1}{g_1} = \frac{V_1 \sin B_1}{R_s \cos \lambda_1 - R_0} \tag{2}$$

where

V = speed of satellite;
f = horizontal component of slant range;
R_s = distance from center of earth to satellite;
λ = angle between station and satellite, measured at center of earth;
g = vertical component of slant range;
B = azimuth pointing direction of satellite's velocity vector;
R_0 = radius of the earth.

The magnitude of the elevation angle to the satellite at time t_1 may, of course, be computed from the triangle defined by R_0, λ_1 and R_s. From Equations 1 and 2, it is evident that, at the time depicted by Figures 1 and 2, the primary-axis shafts are moving at the maximum speeds required by the particular passes shown.

APPROXIMATION TO PRIMARY SHAFT MOTION

An approximation to the motion of a satellite relative to an X axis and an azimuth axis is shown in Figure 3. In this approximation, it is assumed that the satellite is traveling at a fixed speed V in an eastward direction, and that this direction of travel does not change as a function of time, i.e., it is assumed that the north and vertical components of slant range do not change during the pass. From the top view, it is evident that the required azimuth speed $(\dot{A})$ is a maximum at time t_1 and that

$$\dot{A}_{max} = \frac{V}{f_1} = \frac{V}{S_1 \sin \gamma_1} \tag{3}$$

At time $t_1 + \Delta t$, the satellite has reached a point defined by the azimuth angle A in the top view. It is evident that

$$A = \tan^{-1}\left[\frac{V(\Delta t)}{S_1 \sin \gamma_1}\right] = \tan^{-1}\left[\dot{A}_{max}\,(\Delta t)\right] \tag{4}$$

and that the azimuth speed at time $t_1 + \Delta t$ is

$$\dot{A} = \frac{V \cos A}{S_1 \sin \gamma_1 \sec A} = \dot{A}_{max} \cos^2 A\,. \tag{5}$$

Similarly,

$$X = \tan^{-1}\left[\dot{X}_{max}\,(\Delta t)\right] \tag{6}$$

and

$$\dot{X} = \dot{X}_{max} \cos^2 X \ . \tag{7}$$

It is shown in Appendix A that Equations 4 to 7 are reasonably accurate expressions for the required motions of azimuth and X axes when tracking satellites on passes which require relatively high maximum shaft speeds (3 deg/sec or greater). Since Equation 6 is similar to Equation 4 and Equation 7 is similar to Equation 5, we can write the generalized expressions

$$\phi = \tan^{-1} \left(\dot{\phi}_{max}\right) t \tag{8}$$

and

$$\dot{\phi} = \dot{\phi}_{max} \cos^2 \phi \tag{9}$$

where ϕ and $\dot{\phi}$ are the required position and speed of the primary-axis shaft of any two-axis mount, and where ϕ and t are measured from the position and time at which the satellite is at its minimum distance from the primary axis.**

**It may be noted that the primary shaft acceleration is $\ddot{\phi} = -2\dot{\phi}_{max}\dot{\phi}\cos\phi\sin\phi = -2\left(\dot{\phi}_{max}\right)^2\cos^3\phi\sin\phi$ from which it can be shown that $|\ddot{\phi}|$ reaches a maximum at $\phi = \pm 30°$ and that $|\ddot{\phi}_{max}| = 3\sqrt{3}/8\left(\dot{\phi}_{max}\right)^2$ rad/sec^2 where $\dot{\phi}_{max}$ is expressed in rad/sec.

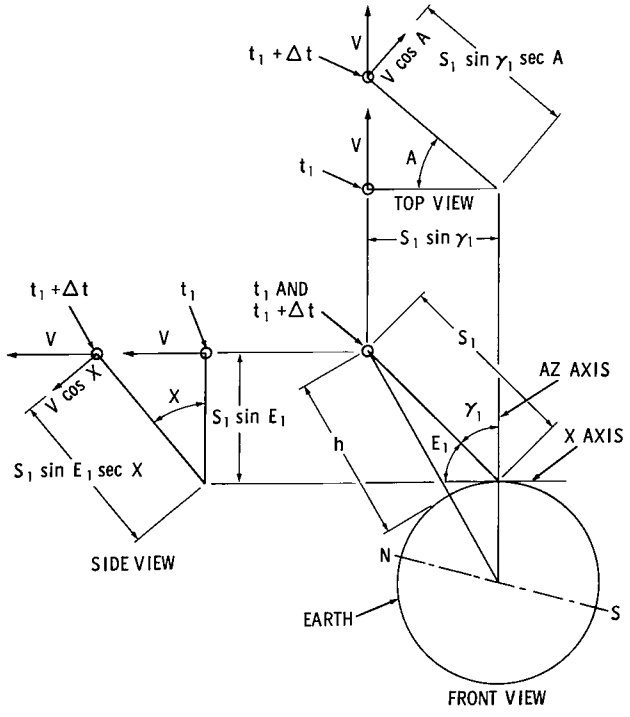

Figure 3—Approximation to motion of a satellite

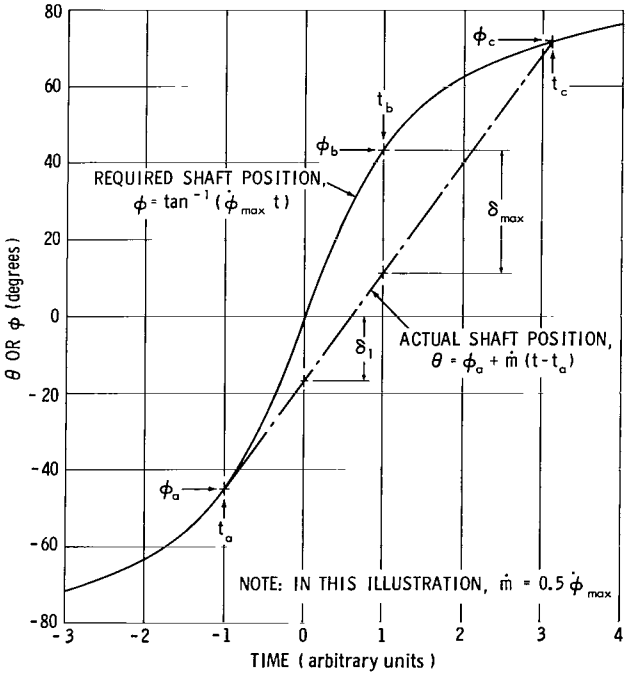

Figure 4—Lag of primary axis.

LAG OF PRIMARY AXIS

Let the maximum speed capability of a primary axis shaft be $\dot{m}$. Let it be assumed that, on a particular pass, the required motion of the shaft is described by Equations 8 and 9, and that $\dot{m} < \dot{\phi}_{max}$. As the satellite comes up over the horizon, $\dot{\phi}$ is small (i.e., $\dot{\phi} < \dot{m}$), so the antenna can at first track the satellite. But as illustrated in Figure 4, the primary axis shaft starts to lag behind its required position at time t_a, when $\dot{\phi} = \dot{m}$. From Equation 9, the shaft angle at this time is

$$\phi_a = -\cos^{-1}\sqrt{\frac{\dot{m}}{\dot{\phi}_{max}}} \tag{10}$$

and, from Equation 8, the time at which the lag begins is

$$t_a = \frac{\tan \phi_a}{\dot{\phi}_{max}} \tag{11}$$

Let it be assumed that the shaft continues to move at the rate $\dot{m}$, as shown in Figure 4. This assumption is generally valid in the practical case wherein the error signal is provided by the tracking receivers while the satellite remains in the main antenna beam, and the error signal is provided by the antenna programmer while the satellite is outside the main beam. If the operational mode is not shifted to the programmer before the satellite leaves the main beam, the assumption is invalid, and the coverage for the pass ceases entirely at the time the satellite leaves the beam. But if the shift to the programmer is made before the satellite leaves the beam, the actual shaft position after time t_a is

$$\theta = \phi_a + \dot{m}\,(t - t_a) \tag{12}$$

and the angle by which the shaft lags behind its required position is

$$\delta = \phi - \theta \tag{13}$$

At time $t = 0$, when $\phi = 0$, the lag is, from Equations 12 and 13,

$$\delta_1 = \dot{m}\, t_a - \phi_a \tag{14}$$

From Figure 4, it is evident that the general expression for lag can also be written as

$$\delta = \phi + \delta_1 - \dot{m}t$$

$$= \phi + \delta_1 - \dot{m}\frac{\tan \phi}{\dot{\phi}_{max}} \tag{15}$$

From Equation 15, it can be shown that δ is a maximum when the satellite is at position $\phi_b = |\phi_a|$, and that

$$\delta_{max} = 2\,\delta_1 \tag{16}$$

The value of ϕ_c, the point at which the antenna overtakes the satellite, may be found from Equation 15 by setting δ equal to zero and using the cut and try method.

LOSS OF COVERAGE DUE TO EXCESSIVE SPEED REQUIREMENTS

From Figure 4, it is evident that the coverage is lost between times t_a and t_c; i.e., between shaft angles ϕ_a and ϕ_c. The satellite position at times t_a and t_c can be described in terms of the east, north and vertical components of the slant range. For satellites traveling in the manner depicted in Figure 3, the north and vertical components are assumed to be constant during a pass which crosses the meridian at any selected elevation angle, and the east components at times t_a and t_c in the pass are

$$EAST_a = f_1 \tan A_a$$

or

$$EAST_a = g_1 \tan X_a$$

and

$$EAST_c = f_1 \tan A_c$$

or

$$EAST_c = g_1 \tan X_c$$

The east and north components at times t_a and t_c, calculated for a number of passes and normalized to the horizon distance D, may be plotted on a horizon-plane view, where the enclosed area represents the loss of coverage. Such diagrams are shown in Figures 5 and 6, for satellites in circular orbits at heights of 100 and 600 nautical miles, for maximum speed capabilities of $\dot{m} = 3$ deg/sec on both the azimuth and X axes. In Figure 5, the loss of coverage of the X-Y mount is shown for $B_1 = 90°$, $60°$, $45°$ and $30°$; for $B_1 < 90°$, the values of $EAST_a$ and $EAST_c$ were computed by assuming that the satellite was traveling from west to east, but at a reduced speed V sin B_1.

LOSS OF COVERAGE DUE TO LIMIT STOPS

Some X-Y mounts, such as those used with the NASA Range and Range Rate X-Y antennas, are capable of pointing in any direction within the hemisphere above 0° elevation. But other X-Y

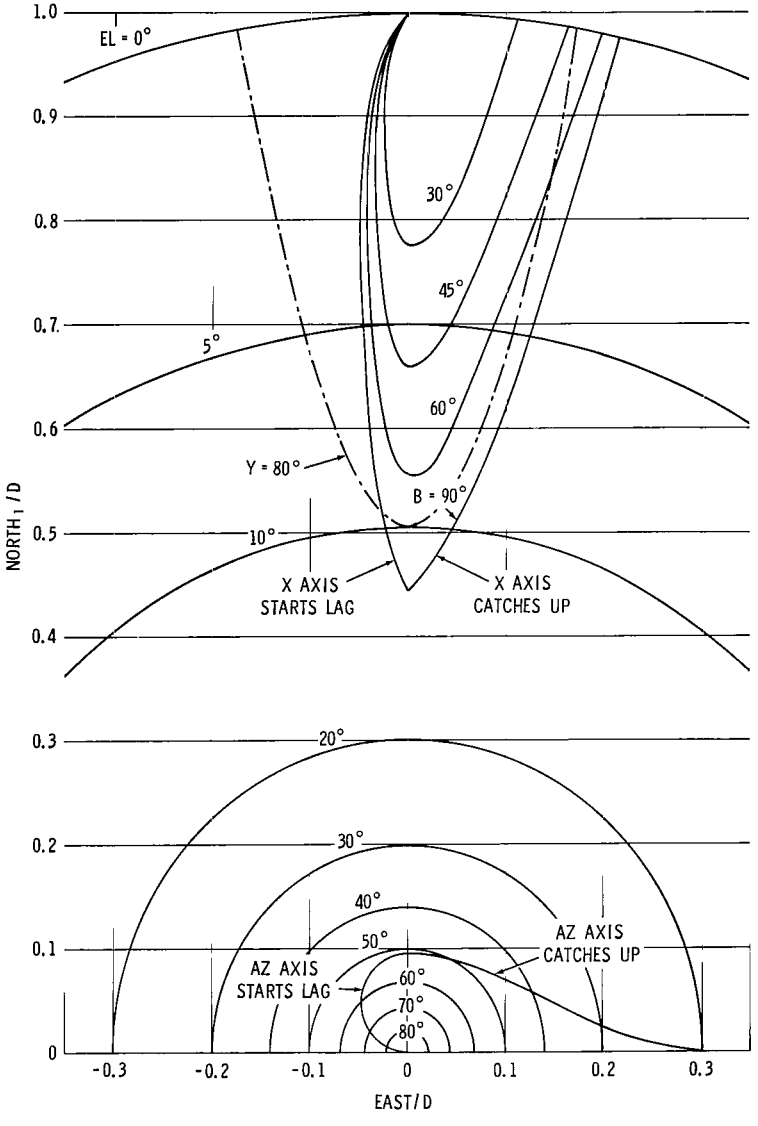

Figure 5–Coverage diagram for 100 n. mi. circular orbit; west-to-east passes; shaft speed capability of 3 deg/sec.

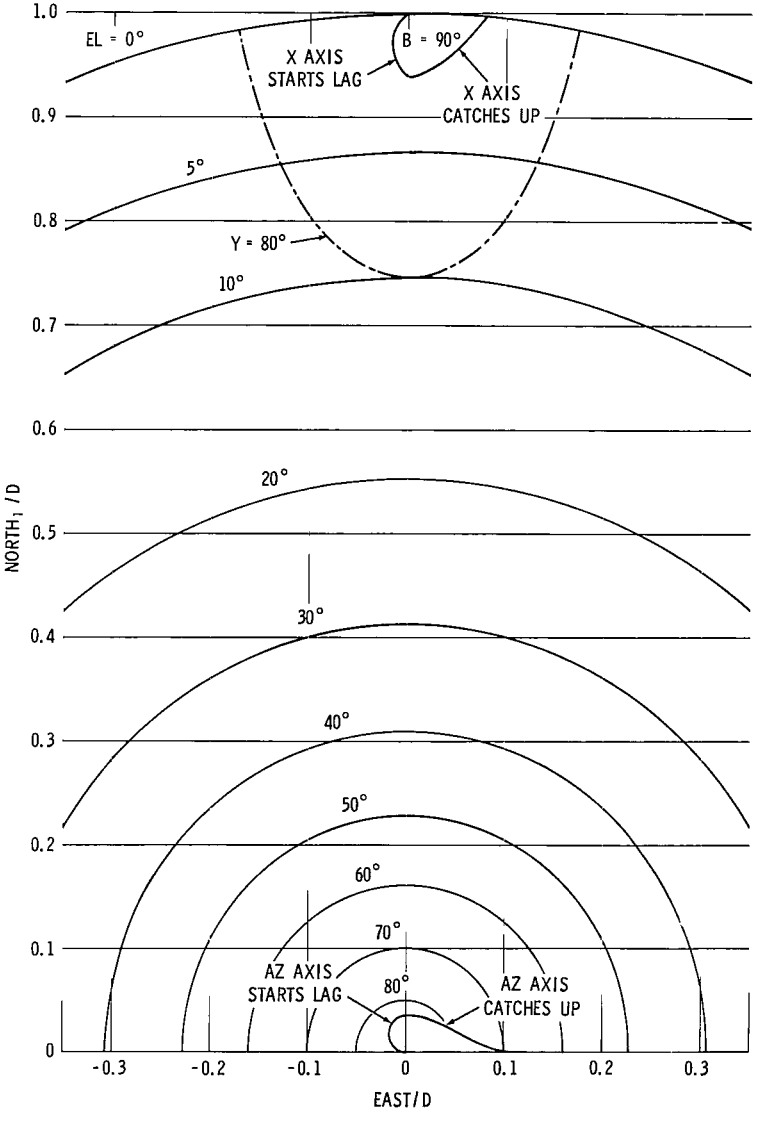

Figure 6–Coverage diagram for 600 n. mi. circular orbit; west-to-east passes; shaft speed capability of 3 deg/sec.

mounts, such as those used with the NASA 85-foot dishes, have electrical or mechanical stops which limit the possible scanning motions to less than a full hemisphere. The loss of coverage due to such stops at $Y = \pm 80°$ are shown in Figures 5 and 6 for the 100 and 600 n. mi. satellites.

DISCUSSION

The coverage lost due either to excessive speed requirements, or to the use of limit stops, may be expressed as a percentage of the total area of the horizon circle at 0° elevation. However, local terrain shielding, ground reflections, refraction, and great atmospheric attenuation all conspire to make data taken at low elevation angles less than useful; hence, the loss expressed as a percentage of the area above the 5° horizon is more meaningful.

The losses of an X-Y mount due to excessive speed requirements, for a 100 n. mi. orbit and for $\dot{m} = 3$ deg/sec, are plotted in Figure 7, as a function of the angle B_1. The loss relative to the 5° horizon, averaged over all values of B_1 from 0° to 90°, is only about 1.3 percent.

The losses of an AZ-EL mount due to shaft speed requirements greater than 3 deg/sec, and the losses of an X-Y mount due to limit stops at $Y = \pm 80°$ are shown in Figure 8, where the losses are normalized to the area of a 5° horizon circle.

The losses of coverage of AZ-EL and X-Y mounts, for $\dot{m} = 3$ deg/sec and for satellites at heights of 100 and 600 n. mi. are given in Tables 1 and 2. As indicated previously, the losses tabulated for the 0° horizon are of much less significance than those tabulated for the 5°

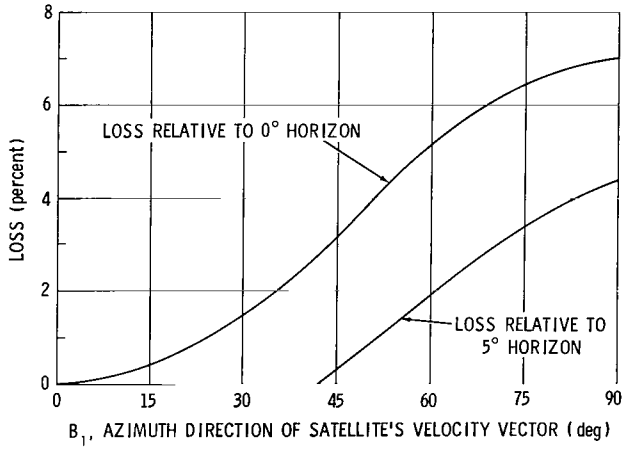

Figure 7—Loss of coverage for X-Y mount due to shaft speed requirements greater than 3 deg/sec; 100 n. mi. orbit.

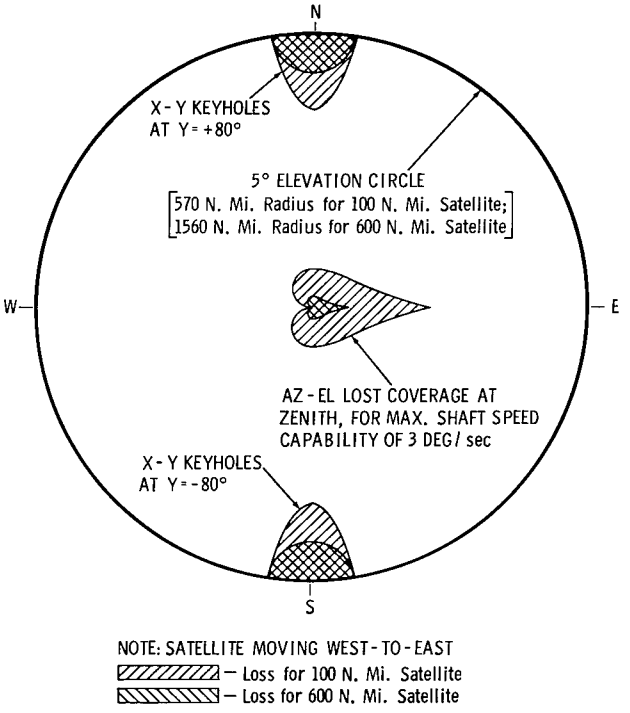

Figure 8—Losses of coverage relative to 5° horizon.

Table 1

Loss of Coverage for 100 n. mi. Circular Orbits

Cause of Loss	Loss, Percent of Area above 0° and 5° Horizons	
	0° Horizon	5° Horizon
$\dot{A}$ > 3 deg/sec	1.2	2.4
$\dot{X}$ > 3 deg/sec, B_1 = 90°	7.0	4.4
$\dot{X}$ > 3 deg/sec, avg. for all possible values of B_1.	3.3	1.3
Y limit = ±80°	8.6	4.2

Table 2

Loss of Coverage for 600 n. mi. Circular Orbits

Cause of Loss	Loss, Percent of Area above 0° and 5° Horizons	
	0° Horizon	5° Horizon
$\dot{A}$ > 3 deg/sec	0.16	0.21
$\dot{X}$ > 3 deg/sec, B_1 = 90°	0.2	ZERO
Y limit = ±80°	4.4	2.1

horizon. For the 100 n. mi. orbits and the 5° horizon, the X-Y mount's loss of coverage due to excessive speed requirements, averaged over all values of B_1, is less than the AZ-EL mount's loss due to this cause. For the 600 n. mi. orbits and the 5° horizon, the X-Y mount has no loss of coverage due to excessive speed requirements, and the loss of the AZ-EL mount is so small (0.21%) that it may be considered to be negligible. For both orbital heights, limit stops at Y = ±80° (if they existed) would be the dominant factor affecting the X-Y mount's loss of coverage.

The significant difference between AZ-EL and X-Y mounts lies not in the fact that one has a much greater percentage loss of coverage due to excessive shaft speed requirements, but in the fact that the information lost by the X-Y mount is of relatively poor quality, while that lost by the AZ-EL mount is of the best quality.

As a corollary point of interest, consideration might be given to selection of the antenna elevation angle for optimizing reflector distortion and minimizing feed sag. The most general conditions for orbit inclination and station location make it factual that a near-earth satellite may be at any point within the antenna coverage circle with equal probability. The elevation angle to be selected for best antenna adjustment might be taken as the one corresponding to a satellite with a horizontal range equal to 0.707 times the radius of the coverage circle at 5° elevation; there would then be equal probabilities for the satellite to be above or below the best-adjustment

elevation angle. For the two cases of satellites at heights of 100 and 600 nautical miles, these elevation angles are 11° and 17° respectively. Other factors to be considered are the facts that (1) the antenna gain requirement increases (for any given orbit height) as the elevation angle decreases and the slant range simultaneously increases; and (2) the gain requirement also increases (for any given elevation angle) as the orbit height increases. For a general-purpose antenna intended for use in tracking a wide variety of near-earth satellites (as differentiated from probes), it appears that the antenna reflector distortion and the feed sag should be minimized at approximately 20° elevation angle.

(Manuscript received December 24, 1964)

Appendix A

Accuracy of Approximation for Primary Axis Motion

In the main body of this paper, Equations 8 and 9 describe the required position and speed of the primary axis of any two-axis antenna which is tracking a satellite traveling in the manner depicted in Figure 3; the equation for shaft acceleration is given in a footnote. Without loss of generality, the equations can be considered to be approximate expressions for the required motion of the primary axis of an antenna which is tracking an actual satellite, and can be written as

$$\phi \approx \tan^{-1}\left(\dot{\phi}_{max}\right)t \ ,$$

$$\dot{\phi} \approx \dot{\phi}_{max} \cos^2 \phi \ ,$$

$$\ddot{\phi} \approx -2\left(\dot{\phi}_{max}\right)^2 \cos^3 \phi \sin \phi$$

where ϕ and t are measured, respectively, from the primary-axis position and the time at which the satellite is at its point of closest approach to the axis.

Actual values of required shaft position, speed and acceleration for six selected passes of circular-orbit satellites have been compared with approximate values calculated from the above expressions. The actual values of shaft position and speed were computed on IBM 7090 equipment, using Goddard Space Flight Center's normal satellite prediction programs; these values were computed for one-second intervals of time during the pass, but were printed out only for each alternate second. The shaft acceleration was also computed and printed by the IBM 7090 equipment, but was calculated from a simple straight-line formula; that is, the acceleration was taken as the average change in actual shaft speed during the two-second interval bracketing the print-out time. On each of the actual passes, the satellite's velocity vector was pointing nearly due east or west at the time of closest approach to the primary axis.*

On three of the selected passes, data was printed out for X-axis motion, and on the other three the data was printed out for azimuth-axis motion. The passes are identified as follows:

Pass No.	Axis	Max. Shaft Speed, deg/sec
X-0.8	X	0.77526
A-0.8	Azimuth	0.77519
X-2.9	X	2.94901
A-2.9	Azimuth	2.89824
X-8.6	X	8.61980
A-8.1	Azimuth	8.08724

*The satellites and the tracking stations were "actual" only in the sense that normal computer programs were used in producing the data.

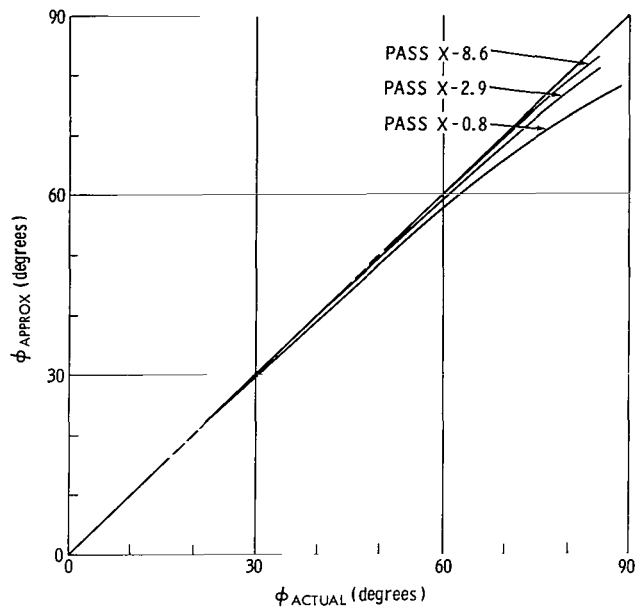

Figure A-1—Actual and approximate shaft positions, X-axis passes.

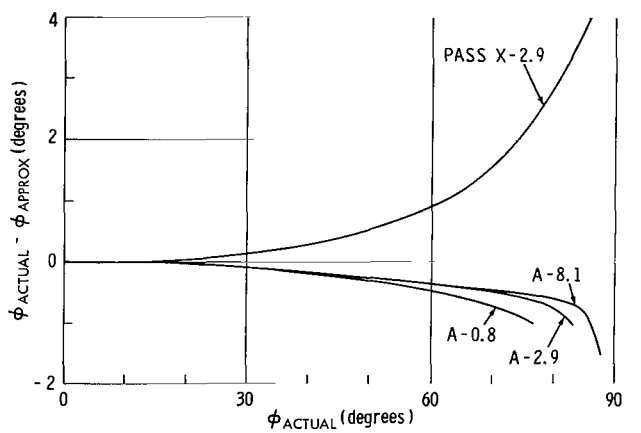

Figure A-2—Difference between actual and approximate shaft positions, azimuth-axis passes.

In Figure A-1, the approximate value of ϕ is plotted against the actual value of ϕ, for the three X-axis passes. It may be noted that the accuracy of the approximation is good for the passes on which the maximum shaft speed is relatively high.

It was found that the accuracy of the approximation is, in general, better for an azimuth-axis pass than for an X-axis pass requiring approximately the same maximum shaft speed. For the azimuth-axis passes, it is impractical to plot the approximate value of ϕ against the actual value on a chart of the same scale as Figure A-1; therefore, the difference between the actual and approximate values is shown in Figure A-2, along with the difference for Pass X-2.9 which is shown for reference.

In Figure A-3, normalized values of the approximate and actual shaft speeds are shown for the X-axis passes. In Figure A-4, the difference between the normalized actual and approximate speeds is shown for the azimuth-axis passes; a curve for Pass X-2.9 is again included for reference.

From the characteristics of the curves in Figures A-1 through A-4, it is concluded that the approximate expressions for shaft position and shaft speed are sufficiently accurate for the purposes for which they were used in this paper, i.e., calculating the losses of coverage for X-Y and elevation-over-azimuth antenna mounts which have maximum speed capabilities of 3 deg/sec.

In Figure A-5, normalized values of the approximate and actual shaft accelerations are shown for the X-axis passes. On the curve for Pass X-8.6, the available data points (printed out for two-second intervals) are circled and are connected by a dash-dot line; in terms of the independent variable ϕ, these points are so far apart that it is impractical to draw a smooth curve connecting them. In Figure A-6, the difference between the approximate and actual normalized accelerations is shown for the azimuth-axis passes, and a curve for Pass X-2.9 is again included for reference.

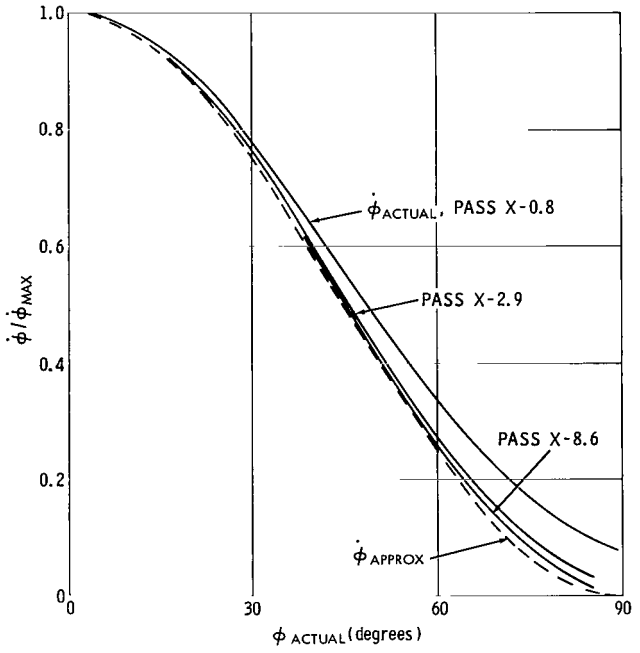

Figure A-3—Actual and approximate shaft speeds, X-axis passes.

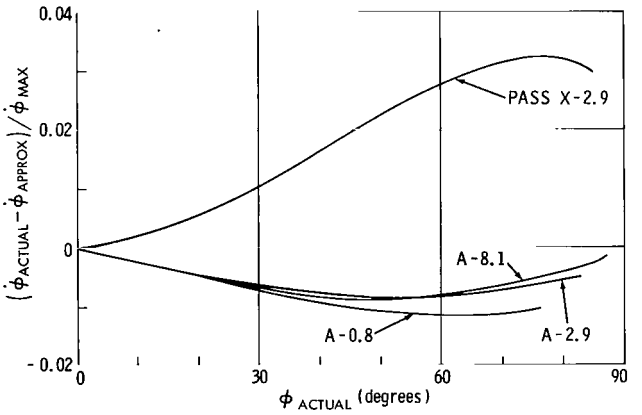

Figure A-4—Difference between actual and approximate shaft speeds, azimuth-axis passes.

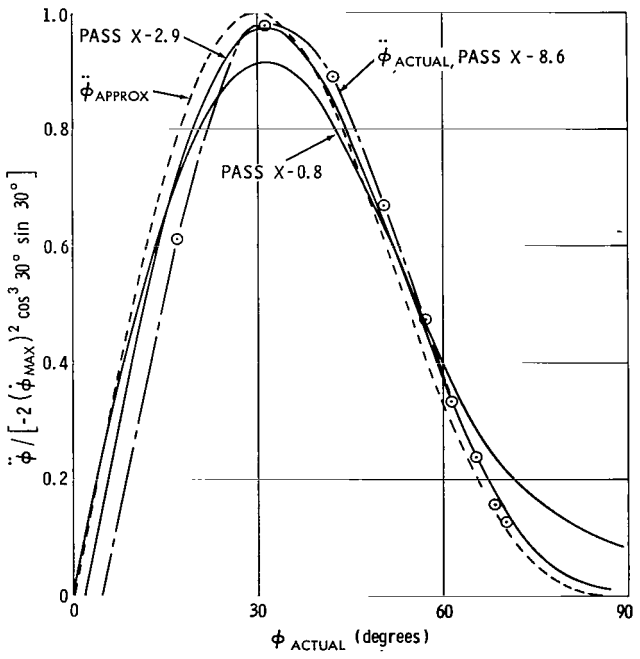

Figure A-5—Actual and approximate shaft accelerations, X-axis passes.

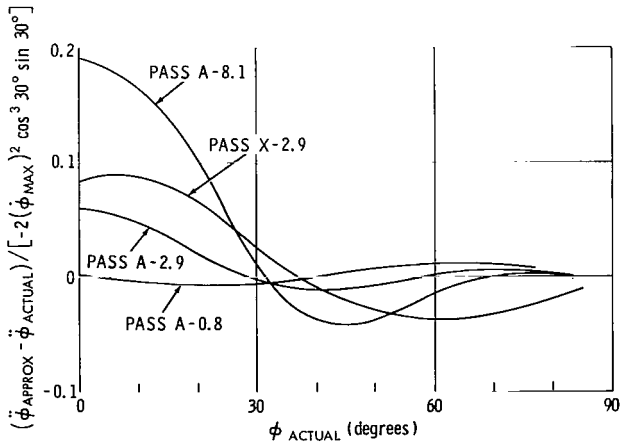

Figure A-6—Difference between actual and approximate shaft accelerations, azimuth-axis passes.

Figures A-1 through A-4 indicate that when the actual value of ϕ is small (i.e., less than about 20 degrees), the approximations for shaft position and shaft speed are quite accurate. From this fact, it could be inferred that the approximation for shaft acceleration should also be quite accurate when ϕ is small; but Figures A-5 and A-6 seem to refute such an inference, especially on Passes X-8.6 and A-8.1. It is believed that the "actual" accelerations, printed out from the IBM 7090 data, are not very accurate in the region near $\phi = 0°$ because the computer program for accelerations assumes that the change in speed is essentially linear during a two-second interval of time, while in fact, as may be noted from Figure A-3, the change in speed near $\phi = 0°$ is not really linear over the large increment of ϕ which, on a high-speed pass, corresponds to a small (two-second) increment of time. It is concluded that the differences between the "actual" and approximate values of acceleration, shown in Figures A-5 and A-6, are probably not very accurate in the region near $\phi = 0°$, especially for the passes requiring high shaft speeds.

At values of ϕ greater than about 20°, the IBM 7090 values of shaft acceleration are probably quite accurate because the speed curves in Figure 3 become relatively linear and because the increment of ϕ corresponding to a two-second increment of time becomes progressively smaller.

From Figures A-5 and A-6, it may be noted that, at $\phi = 30°$, there is only a small difference between the actual and approximate values of shaft acceleration. Since this is the point where the approximate value of acceleration is a maximum, it is concluded that the approximate value can be used as a reasonably accurate estimate of the actual maximum acceleration required on any satellite pass which requires a maximum shaft speed of 3 deg/sec or greater.

It should be noted that the magnitudes of the maximum accelerations given by either the approximation, or by a computer program as described above, are quite small. For example, if the maximum shaft speed is 3 deg/sec (i.e., $\pi/60$ rad/sec), then

$$\ddot{\phi}_{max} \approx \left[\frac{3\sqrt{3}}{8}\left(\frac{\pi}{60}\right)^2 \text{ rad/sec}^2\right]\frac{180}{\pi} \text{ deg/rad}$$

$$\approx 0.102 \text{ deg/sec}^2$$

In practice, an antenna mount having a maximum speed capability of 3 deg/sec would be designed to have a maximum acceleration capability much greater than 0.1 deg/sec^2, because high accelerations are required to initially lock on to a moving target and to maintain small tracking errors during the pass.

"The aeronautical and space activities of the United States shall be conducted so as to contribute . . . to the expansion of human knowledge of phenomena in the atmosphere and space. The Administration shall provide for the widest practicable and appropriate dissemination of information concerning its activities and the results thereof."

—NATIONAL AERONAUTICS AND SPACE ACT OF 1958

NASA SCIENTIFIC AND TECHNICAL PUBLICATIONS

TECHNICAL REPORTS: Scientific and technical information considered important, complete, and a lasting contribution to existing knowledge.

TECHNICAL NOTES: Information less broad in scope but nevertheless of importance as a contribution to existing knowledge.

TECHNICAL MEMORANDUMS: Information receiving limited distribution because of preliminary data, security classification, or other reasons.

CONTRACTOR REPORTS: Technical information generated in connection with a NASA contract or grant and released under NASA auspices.

TECHNICAL TRANSLATIONS: Information published in a foreign language considered to merit NASA distribution in English.

TECHNICAL REPRINTS: Information derived from NASA activities and initially published in the form of journal articles.

SPECIAL PUBLICATIONS: Information derived from or of value to NASA activities but not necessarily reporting the results of individual NASA-programmed scientific efforts. Publications include conference proceedings, monographs, data compilations, handbooks, sourcebooks, and special bibliographies.

Details on the availability of these publications may be obtained from:

SCIENTIFIC AND TECHNICAL INFORMATION DIVISION

NATIONAL AERONAUTICS AND SPACE ADMINISTRATION

Washington, D.C. 20546